J. Appl. Comput. Mech., 6(SI) (2020) 1168-1177
DOI: 10.22055/JACM.2020.32136.1973

ISSN: 2383-4536
jacm.scu.ac.ir

Shahid Chamran University of Ahvaz

Journal of Applied and Computational Mechanics

Research Paper

Unsteady Stokes Flow through a Porous Pipe with Periodic Suction and Injection with Slip Conditions

Zarqa Bano[1], Abdul Majeed Siddiqui[2], Kaleemullah Bhatti[1]

[1] Department of Mathematics and Social Sciences, Sukkur IBA University, Airport Road Sukkur, 65200, Pakistan, Email: zarqa.bano@iba-suk.edu.pk, kaleem.msmts@iba-suk.edu.pk

[2] Department of Mathematics (York Campus), Pennsylvania State University, York, PA 17403, USA, Email: ams5@psu.edu

Received January 02 2020; Revised March 20 2020; Accepted for publication April 10 2020.
Corresponding author: Kaleemullah Bhatti (kaleem.msmts@iba-suk.edu.pk)

Abstract. The problem of unsteady Stokes flow of certain Newtonian fluids in a circular pipe of uniform cross section is discussed. The pipe is uniformly porous. The unsteady Navier-Stokes equations for the system in cylindrical polar coordinates have been solved analytically to obtain a complete description of the flow. The solution of the flow equations subject to the slip boundary conditions leads to the detailed expressions for axial and radial components of velocity and the pressure distribution depending on position coordinates and time. As a special case we have presented the situation when no-slip boundary conditions are implemented. The velocity profile is analyzed for different values of the flow parameters like Womersley number, slip length and time.

Keywords: Hydrodynamics, Porous Channel, Periodic Suction and Injection, Slippage Effects.

1. Introduction

Stokes flow or creeping motion is the flow of fluids where viscous forces are highly dominating as compared to the inertial forces resulting low Reynolds number Re<<1. In such situations, fluid velocities are very small and viscosity is high. Initially such types of flows were studied in order to understand the process of lubrication of engines. Stokes flows also occur in nature in swimming of microorganism and sperm and flow of lava. The equations governing such flows are called Stokes equations and are linearized form of the well-known Navier-Stokes equations.

In this paper we have considered a porous circular pipe in which a laminar flow occurs and the fluid layer in contact with the wall of the pipe has some non-zero velocity. At the same time there is periodic suction or injection of the fluid through the pores. There are many real-life applications that correspond to laminar flow through various porous geometries. One of such applications is the modeling of transpiration cooling process in which a cooling fluid is injected in order to protect the walls of a certain engine from the heat.

The problem of laminar flow through a porous channel was firstly studied by Abraham S. Berman in 1953 [1]. He considered the flow through a rectangular channel. There was uniform suction through the upper face and uniform injection through the lower face of the channel. Berman investigated in detail the effect of wall porosity on the two-dimensional steady-state incompressible laminar flow of a fluid by solving Navier-Stokes Equations. After that many attempts have been made to solve such type of problems subject to various conditions. In [5], authors studied Berman's problem for a non-Newtonian fluid. In [3], authors encountered the Stokes and Couette flows produced due to oscillatory motion of a wall. In such situations no-slip condition is no longer valid. In [6], Ganesh studied unsteady Stokes flow through a channel of parallel porous plates when there is periodic suction through the lower plate and periodic injection through the upper plate. Kirubhashankar et al. [2] slightly modified this problem for an unsteady MHD flow between two parallel plates when an external uniform field is applied parallel to the plates. In [4] the authors considered Stokes flow of a Newtonian fluid through a porous pipe of uniform circular cross section with no-slip boundary conditions.

In this paper we have considered the problem of Stokes flow of Newtonian fluid through a uniformly porous pipe. The Navier slip condition is widely used by many authors ([3], [7], [10] and references in these articles) which states that the relative velocity of the fluid with the wall is proportional to the shear rate at the wall. Mathematically this can be expressed as

$$u(x,R)-u_W=\lambda\left|\frac{\partial u}{\partial r}\right|_{r=a}$$

where u_W is velocity of the wall, a is radius of pipe and λ is slip parameter known as "slip length". In this article we have used Navier slip condition at the wall and observed that there are significant changes in the flow behavior with the change in the value of the slip parameter. The Solution is analyzed for different other flow parameters as well. We have presented the no-slip Stokes flow problem studied in [4] as a particular case in this paper.

Published online: April 11 2020

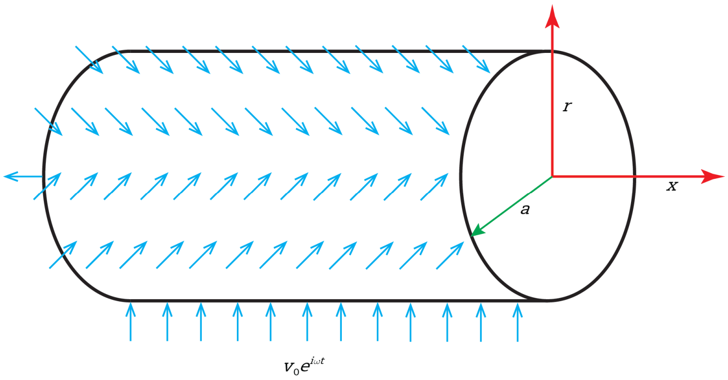

Fig. 1. Schematic diagram the system

2. Problem Formulation

We consider a pipe of uniform circular cross section having infinite length and a Newtonian fluid passes through the pipe. The flow satisfies following assumptions:

- Flow is unsteady and axisymmetric with negligible body forces.
- Stokes flow is assumed. Due to very small Reynolds number the governing equations are simplified by neglecting the convective forces.
- The walls of the pipe are uniformly porous.
- The suction or injection occurs periodically through walls with velocity $v_0e^{i\omega t}$.
- Fluid layer in contact with walls of the pipe has some non-zero velocity called "slip velocity".

In such a situation cylindrical polar coordinates (r,θ,x) are best suited, where X-axis is along the axial axis of pipe and r denotes radial distance from X-axis. Due to axial symmetry θ coordinate vanishes. We chose velocity vector $\vec{U}$ and pressure P in the form

$$\vec{U} = \{u(x,\xi)\hat{i} + v(x,\xi)\hat{j}\}e^{i\omega t}, \tag{1}$$

$$P = p(x,\xi)e^{i\omega t}, \tag{2}$$

where $\xi = r/a$, $(0 \le \xi \le 1)$ and a is radius of the pipe. The equations governing the flow are as given as follows [4]

x **-Component:**

$$i\omega u = -\frac{1}{\rho}\frac{\partial p}{\partial x} + \vartheta\left(\frac{\partial^2 u}{\partial x^2} + \frac{1}{a^2}\frac{\partial^2 u}{\partial \xi^2} + \frac{1}{a^2\xi}\frac{\partial u}{\partial \xi}\right), \tag{3}$$

r **-Component:**

$$i\omega v = -\frac{1}{a\rho}\frac{\partial p}{\partial \xi} + \vartheta\left(\frac{\partial^2 v}{\partial x^2} + \frac{1}{a^2}\frac{\partial}{\partial \xi}\left(\frac{1}{\xi}\frac{\partial}{\partial \xi}(\xi v)\right)\right), \tag{4}$$

Continuity:

$$\frac{\partial}{\partial x}(\xi u) + \frac{1}{a}\frac{\partial}{\partial \xi}(\xi v) = 0, \tag{5}$$

where u and v are respectively the velocity components in x and r direction of the flow field. The boundary conditions of the flow at any time t are

$$u(x,1) = \lambda\left|\frac{\partial u}{\partial \xi}\right|_{\xi=1}, \tag{6}$$

$$\left(\frac{\partial u}{\partial \xi}\right)_{\xi=0} = 0, \tag{7}$$

$$v(x,0) = 0, \tag{8}$$

$$v(x,1) = v_0. \tag{9}$$

3. Solution of the Problem

We introduce the stream function ψ as follows so that the continuity eq. (5) is identically satisfied

$$u(x,\xi)=\frac{1}{a^2\xi}\frac{\partial\psi}{\partial\xi}, \tag{10}$$

$$v(x,\xi)=-\frac{1}{a\xi}\frac{\partial\psi}{\partial x}. \tag{11}$$

We write the stream function ψ as the product

$$\psi(x,\xi)=g(x)h(\xi). \tag{12}$$

Equations (10) and (11) reduce to

$$u(x,\xi)=\frac{1}{a^2\xi}g(x)h'(\xi), \tag{13}$$

$$v(x,\xi)=-\frac{1}{a\xi}g'(x)h(\xi). \tag{14}$$

The boundary conditions of the problem together with the knowledge of inlet conditions to the pipe gives rise to an expression for $g(x)$

$$g(x)=\frac{1}{h(1)}\left(\frac{a^2u_0}{2}-av_0x\right), \tag{15}$$

where u_0 is the average axial velocity of fluid at the entrance of pipe and is given as

$$u_0=2\int_0^1\xi u(0,\xi)\,d\xi. \tag{16}$$

Further let

$$\phi(\xi)=\frac{h'(\xi)}{\xi h(1)}, \tag{17}$$

and

$$\Phi(\xi)=\frac{h(\xi)}{\xi h(1)}=\frac{1}{\xi}\int_0^\xi t\phi(t)dt. \tag{18}$$

Using eq. (15), eq. (17) and eq. (18) we get the the velocity components as follows

$$u(x,\xi)=\left(\frac{u_0}{2}-\frac{xv_0}{a}\right)\phi(\xi), \tag{19}$$

and

$$v(x,\xi)=v_0\Phi(\xi). \tag{20}$$

The stream function reduces to

$$\psi(x,\xi)=\left(\frac{a^2u_0}{2}-av_0x\right)\xi\Phi(\xi). \tag{21}$$

In above equations the function $\phi(\xi)$ is still to be determined. It is worth to briefly specify here that radial velocity component v has become function of "ξ" only. Using eq. (19) and eq. (20) in eq. (3) and eq. (4) we have

$$-\frac{1}{\rho}\frac{\partial p}{\partial x}=\left(\frac{u_0}{2}-\frac{xv_0}{a}\right)\left(i w\phi(\xi)-\frac{\vartheta}{a^2}\left(\phi''(\xi)+\frac{\phi'(\xi)}{\xi}\right)\right), \tag{22}$$

and

$$-\frac{1}{a\rho}\frac{\partial p}{\partial\xi}=i\omega v_0\Phi(\xi)-\frac{\vartheta v_0}{a^2}\left(\Phi''(\xi)+\frac{\Phi'(\xi)}{\xi}-\frac{\Phi(\xi)}{\xi^2}\right). \tag{23}$$

From here and onward we use the notations ϕ and Φ respectively instead of $\phi(\xi)$ and $\Phi(\xi)$ in order to make the expressions simple. Differentiate eq. (22) with respect to ξ to get

$$-\frac{1}{\rho}\frac{\partial^2 p}{\partial\xi\partial x}=\left(\frac{u_0}{2}-\frac{x}{a}v_0\right)\left(i w\phi'-\frac{\vartheta}{a^2}\left(\phi'''+\frac{\phi''}{\xi}-\frac{\phi'}{\xi^2}\right)\right). \tag{24}$$

Also differentiate eq. (23) with respect to x to get

$$-\frac{1}{\rho}\frac{\partial^2 \rho}{\partial x \partial \xi} = 0. \tag{25}$$

Equating the results of eq. (24) and eq. (25) we have

$$\left(\frac{u_0}{2} - \frac{x}{a}v_0\right)\left(i\omega\phi' - \frac{\vartheta}{a^2}\left(\phi''' + \frac{\phi''}{\xi} - \frac{\phi'}{\xi^2}\right)\right) = 0, \tag{26}$$

since this is to be satisfied for all x , therefore

$$i\omega\phi' - \frac{\vartheta}{a^2}\left(\phi''' + \frac{\phi''}{\xi} - \frac{\phi'}{\xi^2}\right) = 0, \tag{27}$$

with the substitution $\beta^2 = \frac{i\omega}{\vartheta} = \frac{\rho i\omega}{\mu}$ eq. (27) becomes

$$\beta^2 a^2 \phi' - \left(\phi''' + \frac{\phi''}{\xi} - \frac{\phi'}{\xi^2}\right) = 0, \tag{28a}$$

or

$$\phi''' + \frac{\phi''}{\xi} - \left(\frac{1}{\xi^2} + \beta^2 a^2\right)\phi' = 0. \tag{28b}$$

Following boundary conditions on functions ϕ and Φ are obtained using eq. (19), eq. (20) and prescribed boundary conditions eq. (6) to eq. (9)

$$\phi(1) = \lambda\phi'(1), \phi'(0) = 0, \Phi(0) = 0, \Phi(1) = 1 \tag{29}$$

We have the third order linear ordinary differential equation eq. (28) subject to the boundary conditions eq. (29). The general solution of eq. (28) is easily obtained in terms of Modified Bessel functions as

$$\phi(\xi) = c_1 + c_2 I_0(a\beta\xi) + c_3 K_0(a\beta\xi). \tag{30}$$

where $I_\alpha(x)$ and $K_\alpha(x)$ are Modified Bessel functions of first and second kind respectively. These functions are defined as

$$I_\alpha(x) = \sum_{m=0}^{\infty}\frac{1}{m!\Gamma(m+\alpha+1)}\left(\frac{x}{2}\right)^{2m+\alpha},$$

$$K_\alpha(x) = \frac{\pi}{2}\frac{I_{-\alpha}(x) - I_\alpha(x)}{\sin(\pi\alpha)}.$$

Since 1 , $I_0(a\beta\xi)$ and $K_0(a\beta\xi)$ are three linearly independent solutions, therefore we can drop $K_0(a\beta\xi)$ having less contribution in the solution. Also $K_0(a\beta\xi)$ diverges at $\xi = 0$ with singularity of logarithmic type. With this assumption eq. (30) reduces to

$$\phi(\xi) = c_1 + c_2 I_0(a\beta\xi).$$

$$c_1 = \frac{2a\beta(I_0(a\beta) - a\beta\lambda I_1(a\beta))}{a\beta I_0(a\beta) - (a^2\beta^2\lambda + 2)I_1(a\beta)}, \tag{31}$$

$$c_2 = \frac{-2a\beta}{a\beta I_0(a\beta) - (a^2\beta^2\lambda + 2)I_1(a\beta)}.$$

Substitute these constants in eq. (31) to get

$$\phi(\xi) = \frac{2a\beta(I_0(a\beta) - I_0(a\beta\xi) - a\beta\lambda I_1(a\beta))}{a\beta I_0(a\beta) - (a^2\beta^2\lambda + 2)I_1(a\beta)}. \tag{32}$$

And using eq. (32) in eq. (18) we get

$$\Phi(\xi) = \frac{a\beta\xi I_0(a\beta) - 2I_1(a\beta\xi) - a^2\beta^2\lambda\xi I_1(a\beta)}{a\beta I_0(a\beta) - 2I_1(a\beta) - a^2\beta^2\lambda I_1(a\beta)}. \tag{33}$$

Substitute ϕ and Φ from eq. (32) and eq. (33) in the components of velocity eq. (19) and eq. (20) to get

$$u(x,\xi) = \left(\frac{u_0}{2} - \frac{xv_0}{a}\right)\phi(\xi),$$

$$u(x,\xi) = \left(\frac{u_0}{2} - \frac{xv_0}{a}\right)\frac{2a\beta(I_0(a\beta) - I_0(a\beta\xi) - a\beta\lambda I_1(a\beta))}{a\beta I_0(a\beta) - (a^2\beta^2\lambda + 2)I_1(a\beta)}, \tag{34}$$

and

$$\upsilon(x,\xi)=\upsilon_0\Phi(\xi),$$

$$\upsilon(x,\xi)=\upsilon_0\frac{a\beta\xi I_0(a\beta)-2I_1(a\beta\xi)-a^2\beta^2\lambda\xi I_1(a\beta)}{a\beta I_0(a\beta)-2I_1(a\beta)-a^2\beta^2\lambda I_1(a\beta)}. \tag{35}$$

Hence unsteady components of the velocity are

$$u(x,\xi,t)=\left(\frac{u_0}{2}-\frac{x\upsilon_0}{a}\right)\frac{2a\beta(I_0(a\beta)-I_0(a\beta\xi)-a\beta\lambda I_1(a\beta))}{a\beta I_0(a\beta)-(a^2\beta^2\lambda+2)I_1(a\beta)}e^{i\omega t}, \tag{36}$$

and

$$\upsilon(x,\xi,t)=\upsilon_0\frac{a\beta\xi I_0(a\beta)-2I_1(a\beta\xi)-a^2\beta^2\lambda\xi I_1(a\beta)}{a\beta I_0(a\beta)-2I_1(a\beta)-a^2\beta^2\lambda I_1(a\beta)}e^{i\omega t}. \tag{37}$$

Equation (36) and eq. (37) completely define the axial and radial velocity components respectively. Further we introduce the following non-dimensional parameters

$$N_{RE}=\frac{au_0}{\vartheta},$$

$$R=\frac{a\upsilon_0}{\vartheta},$$

and

$$\gamma=a\sqrt{\frac{\rho\omega}{\mu}}=\frac{a\beta}{\sqrt{i}}.$$

where γ is dimensionless frequenccy or Womersley number [8] and $i=\sqrt{-1}$ is imaginary unit. Hence by putting $\tau=\omega t$ and using above dimensionless parameters in eq. (36) and eq. (37) we get the following form of the velocity profile

$$\frac{u(x,\xi,\tau)}{u_0}=\left(\frac{1}{2}-\frac{x}{a}\frac{R}{N_{RE}}\right)\frac{2\gamma\sqrt{i}(I_0(\gamma\sqrt{i})-I_0(\gamma\sqrt{i}\xi)-\gamma\sqrt{i}\lambda I_1(\gamma\sqrt{i}))}{\gamma\sqrt{i}I_0(\gamma\sqrt{i})-(\gamma^2\lambda i+2)I_1(\gamma\sqrt{i})}e^{i\tau}, \tag{38}$$

and

$$\frac{\upsilon(x,\xi,\tau)}{\upsilon_0}=\frac{\gamma\sqrt{i}\xi I_0\gamma\sqrt{i})-2I_1(\gamma\sqrt{i}\,\xi)-\gamma^2 i\lambda\xi I_1(\gamma\sqrt{i})}{\gamma\sqrt{i}I_0(\gamma\sqrt{i})-2I_1(\gamma\sqrt{i})-\gamma^2 i\lambda I_1(\gamma\sqrt{i})}e^{i\tau}. \tag{39}$$

Hence the velocity field is fully defined by equation (38) as axial component and by equation (39) as radial component.

4. The Special Case I: $\lambda=0$

Equation (38) and eq. (39) represent generalized solution to the flow problem. If there is no slip between the wall and fluid particles i.e., put $\lambda=0$ in eq. (38) and eq. (39), we obtain

$$\frac{u(x,\xi,\tau)}{u_0}=\left(\frac{1}{2}-\frac{x}{a}\frac{R}{N_{RE}}\right)\frac{2\gamma\sqrt{i}(I_0(\gamma\sqrt{i})-I_0(\gamma\sqrt{i}\xi))}{\gamma\sqrt{i}I_0(\gamma\sqrt{i})-2I_1(\gamma\sqrt{i})}e^{i\tau}, \tag{40}$$

and

$$\frac{\upsilon(x,\xi,\tau)}{\upsilon_0}=\frac{\gamma\sqrt{i}\xi I_0(\gamma\sqrt{i})-2I_1(\gamma\sqrt{i}\xi)}{\gamma\sqrt{i}I_0(\gamma\sqrt{i})-2I_1(\gamma\sqrt{i})}e^{i\tau}. \tag{41}$$

Equation (40) and eq. (41) exactly match with the analytical solution (equations (51) and (52)) we had previously obtained [4] and therefore it is presented here as a special case to the generalized problem discussed in this paper.

5. The Special Case II: $u_0\neq 0,\ \upsilon_0=0$

When there is no suction/injection at the walls flow becomes one dimensional and is driven solely by periodic pressure gradient. In this case the first part of the solution (eq. (38)) can be regarded as superposition of the well-known pulsatile solution/ Womersley solution [11] of the developed oscillating flow in a pipe of infinite length with slip condition. Thus eq. (38) reduces to

$$\frac{u(x,\xi,\tau)}{u_0}=\frac{\gamma\sqrt{i}(I_0(\gamma\sqrt{i})-I_0\gamma\sqrt{i}\xi)-\gamma\sqrt{i}\lambda I_1(\gamma\sqrt{i}))}{\gamma\sqrt{i}I_0(\gamma\sqrt{i})-(\gamma^2\lambda i+2)I_1(\gamma\sqrt{i})}e^{i\tau}. \tag{42}$$

The dimensional velocity profiles given by eq. (42) are compared according to Womersley number γ for no-slip case in **Fig. 9.**

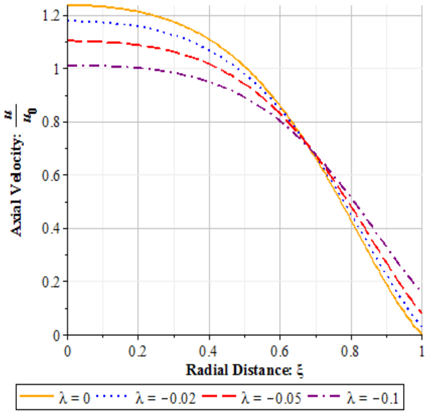

Fig. 2. Axial velocity profile for small suction $R = 1$, $x = 5$, $a = 10$, $\gamma = 5$, $N_{RE} = 10$, $\tau = \pi/4$ and for different values of slip parameter λ.

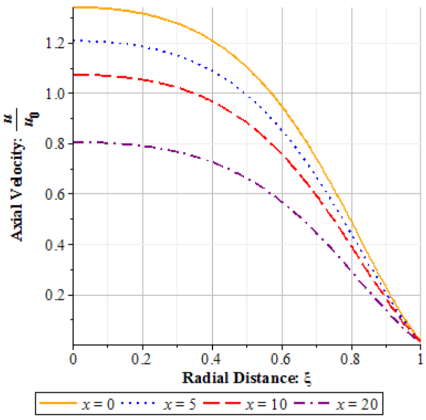

Fig. 3. Axial velocity profile for small suction $R = 1$, $a = 10$, $\gamma = 5$, $N_{RE} = 10$, $\tau = \pi/4$, $\lambda = -0.01$ at different cross sections.

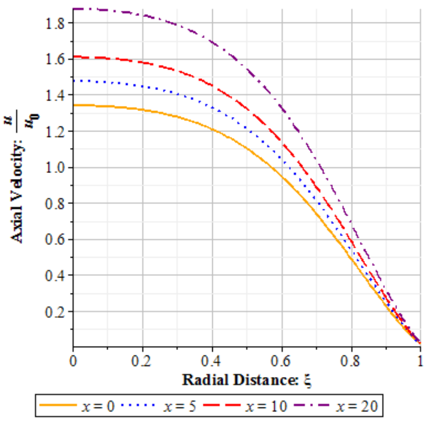

Fig. 4. Axial velocity profile for small injection $R = -1$, $a = 10$, $\gamma = 5$, $N_{RE} = 10$, $\tau = \pi/4$, $\lambda = -0.01$ at different cross sections.

6. Pressure Distribution

The pressure distribution within the flow field can be obtained by extracting the pressure gradients from eq. (22) and eq. (23) and by integrating with respect to x and ξ respectively. Thus we have

$$\int_0^x \frac{\partial p}{\partial x} dx = p(x,\xi) - p(0,\xi), \tag{43}$$

and

$$\int_0^\xi \frac{\partial p}{\partial \xi} d\xi = p(x,\xi) - p(x,0). \tag{44}$$

It follows from eq. (42) and eq. (43) that

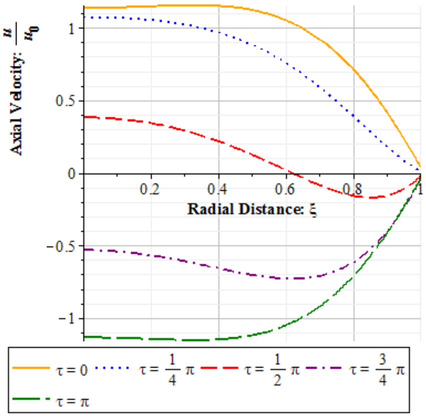

Fig. 5. Axial velocity profile for small suction $R=1$, $x=10$, $a=10$, $\gamma=5$, $N_{RE}=10$, $\lambda=-0.01$ and for different values of τ.

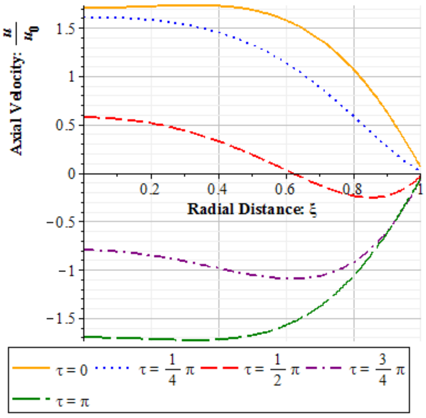

Fig. 6. Axial velocity profile for small injection $R=-1$, $x=10$, $a=10$, $\gamma=5$, $N_{RE}=10$, $\lambda=-0.01$ and for different values of τ.

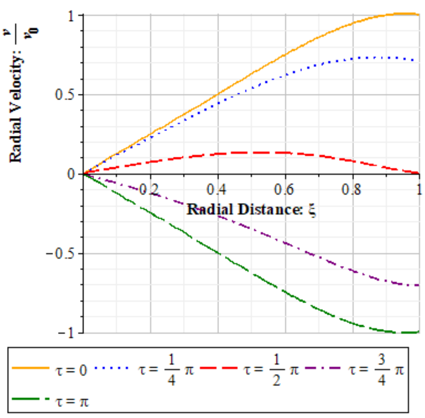

Fig. 7. Radial velocity profile for $\gamma=5$, $\lambda=-0.1$ and for different values of τ.

$$\int_0^x \frac{\partial p}{\partial x}dx + \left(\int_0^\xi \frac{\partial p}{\partial \xi}d\xi\right)_{x=0} = p(x,\xi)-p(0,0). \tag{45}$$

Using eq. (22) and eq. (23) in equation eq. (44) we get

$$\begin{aligned} p(x,\xi) = p(0,0) + \int_0 \mu\left(-a\beta^2 v_0 \Phi(\xi) + \frac{v_0}{a}\left(\frac{d^2}{d\xi^2}\Phi(\xi) + \frac{\frac{d}{d\xi}\Phi(\xi)}{\xi} - \frac{\Phi(\xi)}{\xi^2}\right)\right)d\xi + \frac{1}{2}\frac{\mu v_0 x^2}{a}\left(\beta^2\phi(\xi) - \frac{1}{a^2}\left(\frac{d^2}{d\xi^2}\phi(\xi) + \frac{\frac{d}{d\xi}\phi(\xi)}{\xi}\right)\right) \\ -\frac{1}{2}\mu u_0\left(\beta^2\phi(\xi) - \frac{1}{a^2}\left(\frac{d^2}{d\xi^2}\phi(\xi) + \frac{\frac{d}{d\xi}\phi(\xi)}{\xi}\right)\right)x. \end{aligned} \tag{46}$$

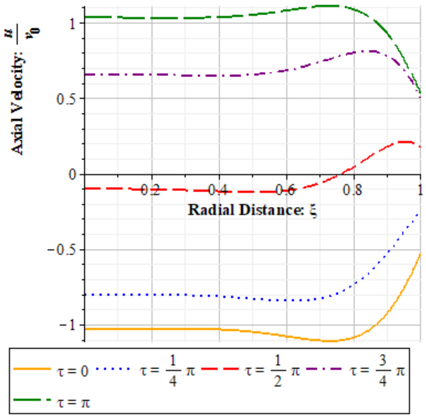

Fig. 8. Axial velocity profile for the case when $u_0 = 0$, $\gamma = 5$, $\lambda = -0.1$, $x = 10$ and for different values of τ.

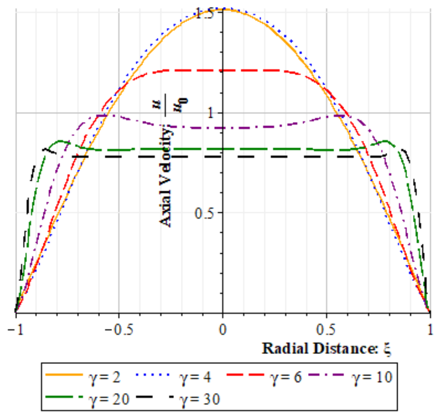

Fig. 9. Dimensionless velocity profiles compared according to Womersley number; $x = 10$, $R = -1$, $a = 10$, $N_{RE} = 3$, $\tau = \pi/4$ and $\lambda = 0$.

Hence from eq. (2) we have

$$P(x,\xi,t) = p(x,\xi)e^{i\omega t}, \tag{47}$$

where $p(0,0)$ is pressure at the entrance of the channel. It is easy to complete the calculation for the pressure distribution by making the substitution for $\phi(\xi)$ and $\Phi(\xi)$ from eq. (32) and eq. (33) in the eq. (45) and eq. (46).

7. Results and Discussion

The expressions for axial and radial velocity components for the two dimensional unsteady stokes flow through a porous pipe of uniform circular cross section have been obtained in eq. (38) and eq. (39) respectively. It was assumed that there is non-zero slip velocity of the fluid layer in contact with the boundary. Hence by discussing special no-slip case we have justified our claim that the problem we have discussed is a generalized version to the one discussed in [4] for $\lambda = 0$.

The curves in **Fig. 2** show the behavior of axial velocity of the fluid for small periodic suction at the cross section $x = 5$ and for four different values of the slip length λ. Near the wall, it was desired to have a direct relationship between the axial velocity of the fluid and slip parameter, which can be visualized clearly in **Fig. 2**. With the increase in numerical value of λ from 0 to 0.1, the magnitude of axial velocity component also increases near the wall. Also the velocity curve for $\lambda = 0$ corresponds to the special no-slip case.

The case when wall Reynolds number is non-negative, corresponds to the periodic suction. The curves in **Fig. 3** show behavior of axial velocity of the fluid for small periodic suction and $\lambda = -0.01$. It has been observed that as fluid passes through various cross sections from $x = 0$ to $x = 20$ the axial velocity decreases. Similarly when wall Reynolds number is negative, precisely $R = -1$, it corresponds to the periodic injection case. The axial velocity increases for this case as fluid passes through various cross sections from $x = 0$ to $x = 20$ which is shown in **Fig. 4**.

In **Fig. 5** and **Fig. 6**, we have the axial velocity plot for small periodic suction and small periodic injection respectively for different values of τ. **Fig. 7** and **Fig. 8** depict the axial and radial velocity profile for the case when $u_0 = 0$ and $v_0 \neq 0$ and for the same values of Womersley number and slip length. It is also worth to note that the axial velocity is greater when τ or $\tau = \pi$ and radial velocity is minimum when $\tau = \pi/2$. In **Fig. 9**, we have the dimesionless axial velocity profiles for six different Womersley numbers from $\gamma = 2$ to $\gamma = 20$. For $\gamma \leq 2$ viscous forces dominate the overall flow. For $\gamma \geq 4$ viscous forces dominate the flow near the boundary layer and inertial forces dominate near the centeral part of the pipe, thus the velocity profile gets flattened near the centeral core.

8. Conclusion

The problem of unsteady Stokes flow of a Newtonian fluid past a porous cylindrical pipe with slip conditions have been discussed. The expressions for velocity components and pressure distribution are obtained. The no-slip case is also reported as a special case of the discussion. The results are hashed out graphically and analyzed by varying values of different parameters involved. It has been found that magnitude of axial velocity component increases with the increase in numerical value of slip parameter. Flow behavior for two different cases of small suction and small injection has also been investigated. It has been observed that for small suction the magnitude of axial velocity component decreases and it increases when there is small injection.

Author Contributions

A.M. Siddiqui identified the problem under discussion; Z. Bano developed the mathematical modeling, examined the theory validation and guided throughout the procedure; K. Bhatti conducted the research and obtained the solutions. The manuscript was written through the contribution of all authors. All authors discussed the results, reviewed and approved the final version of the manuscript.

Acknowledgments

The authors are very grateful to the reviewers for their constructive suggestions and comments. Their comments were very helpful to improve the manuscript. The authors are also thankful to Sukkur IBA University for providing excellent research facilities.

Conflict of Interest

The authors declared no potential conflicts of interest with respect to the research, authorship and publication of this article.

Funding

The authors received no financial support for the research, authorship, and publication of this article.

Nomenclature

u	Velocity along x - direction	x	Coordinate of pipe's longitudinal axis
v	Velocity along r - direction	θ	Coordinate of pipe's azimuthal axis
$\vec{U}$	Unsteady velocity vector	r	Coordinate of pipe's transversal axis
ρ	Constant fluid density	t	Time
a	Radius of the porous pipe	μ	Dynamic viscosity
ξ	Dimension-less radial distance, r/a	ϑ	Kinematic viscosity, μ/ρ
ψ	Stream function	λ	Slip parameter (slip length)
R	Wall Reynolds number [5], $\frac{av_0}{\vartheta}$	$P(x,\xi,t)$	Unsteady pressure distribution at point (x,ξ,t)
u_0	Steady state axial velocity at entrance of pipe $x=0$ averaged over cross-section.	N_{RE}	Reynolds number for flow entering the pipe [5], $\frac{au_0}{\vartheta}$
v_0	Cross flow radial velocity of fluid at wall of the pipe $\xi=1$	$p(x,\xi)$	pressure in the pipe at point (x,ξ)
γ	Dimensionless frequency or Womersley number [8], $a\sqrt{\frac{\rho\omega}{\mu}}$	τ	ωt
β	$\sqrt{\frac{\rho i\omega}{\mu}}$		

References

[1] Berman, A. S., Laminar flow in channels with porous walls, *Journal of Applied Physics*, 24(9), 1953, 1232–1235.
[2] Kirubhashankar, C. K., Ganesh, S., Ismail, A. M., An exact solution of the problem of unsteady MHD flow through parallel porous plates, *International Journal of Advances in Mechanical & Automobile Engineering*, 1, 2014, 39–42.
[3] Khaled, A.-R. A., Wafai, K., The effect of slip condition on Stokes and Couette flows due to an oscillating wall: Exact solutions, *International Journal of Non-Linear Mechanics*, 39(1), 2004, 795-809.
[4] Bano, Z., Bhatti, K., Siddiqui, A. M., Unsteady incompressible Stokes flow through porous pipe of uniform circular cross section with periodic suction and injection, *Sukkur IBA Journal of Computing and Mathematical Sciences*, 1(1), 2017, 13–22.
[5] Narasimhan, M. N. L., Laminar non-Newtonian flow in a porous pipe, *Applied Scientific Research*, 10, 1961, 393-409.
[6] Ganesh, S., Krishnambal, S., Unsteady Stokes flow of viscous fluid between two parallel porous plates, *Journal on Information Sciences and Computing*, 1(1), 2007, 63–66.
[7] Zaman, H., Hall effects on the unsteady incompressible MHD fluid flow with slip conditions and porous walls. *Applied Mathematics and Physics*, 1(2), 2013, 31–38.
[8] Tsangaris, S., Kondaxakis, D., Vlachakis, N. W., Exact solution for flow in a porous pipe with unsteady wall suction and/or injection, *Communications in Nonlinear Science and Numerical Simulation*, 12, 2007, 1181-1189.
[9] Sidnawi, B., Santhanam S., Wu Q., Analytical and numerical study of pulsatile flow in a porous tube, *Journal of Fluid Engineering*, 141, 2019, 121205-1.
[10] Silvia, J. B., Bogdan, V., Derivation of Navier slip and slip length for viscous flows over a rough boundary, *Physics of Fluids*, 29, 2017, 057103.
[11] Womersley, J. R., Method for the calculation of velocity, rate of flow and viscous drag in arteries when the pressure gradient is known, *Journal of Physiology*, 127, 1955, 553-563.

ORCID iD

Zarqa Bano https://orcid.org/0000-0003-2080-8501

Abdul Majeed Siddiqui https://orcid.org/0000-0001-9386-2387
Kaleemullah Bhatti https://orcid.org/0000-0002-0065-0770

How to cite this article: Bano Z., Siddiqui A.M., Bhatti K. Unsteady Stokes Flow through a Porous Pipe with Periodic Suction and Injection with Slip Conditions, *J. Appl. Comput. Mech.*, 6(SI), 2020, 1168–1177. https://doi.org/10.22055/JACM.2020.32136.1973